I-PD CONTROL DESIGN AND ANALYSIS IN AN ISLANDED MICROGRID SYSTEM

S. D. Panjaitan[1], R. Kurnianto[2], B.W. Sanjaya[3], M. C. Turner[4#]

Department of Electrical Engineering, Tanjungpura University, Pontianak 78124, Indonesia

[#] Department of Engineering, University of Leicester, Leicester LE2 1AH, United Kingdom

Emails: seno.panjaitan@ee.untan.ac.id [1], rudi.kurnianto@ee.untan.ac.id [2], bomo.wibowo@ee.untan.ac.id [3], mct6@leicester.ac.uk [4]

Submitted: Aug. 5, 2017 ***Accepted: Nov. 12, 2017*** ***Published: Dec. 1, 2017***

Abstract- Voltage and frequency control is very important especially to face the migration from conventional to smart grid. In conventional way, voltage and frequency are regulated from the main power plant. However, in a smart grid system, the controller can be distributed into sub-system. A microgrid as a key sub-system must have independent control especially in islanded or stand-alone mode. This paper presents an approach named Integral-Proportional Derivative (I-PD) to control the three-phase voltage in a microgrid. In the simulation using MATLAB, a distributed energy resource unit applying voltage-source converter in order to have three-phase voltage from a DC-source is taken into account. Using system identification to simplify the controller design generates a linear model of the system. The compensated system shows a very good reference tracking capability during set point and load changes. It also reduces the coupling effect due to active and reactive power.

Index terms: smart grid, microgrid, voltage control, distributed generator, energy control.

I. INTRODUCTION

The energy conservation focuses on improvement energy efficiency in the users, power plant, and transmission/distribution. Some example works to support energy efficiency can be seen in [1-3] including monitoring system parameters to improve the analysis in the renewable energy [4]. Meanwhile, the improvement of performance in the transmission/distribution now is becoming a challenge with the quite new grid concept named smart grid.

In isolated or communal areas, electricity network for some decades is implemented like small autonomic grids. Renewable distributed generator (RDG) currently grows quite significantly in number and type nowadays. However, integration of RDG unit either with other RDG or main grid shows great challenges to guarantee the system reliability and stability. Problems in interconnection various RDG to supply the demand encourage many engineers and developers to consider smart grid concept and technology as a solution for seamless integration. Those problems are commonly caused by technical or economical reason [5].

A smart grid system involves one or more microgrids as its key component(s). The microgrid is like a distributed resource that may have electricity generation, storage and local loads within a boundary managed by its controller. Two interconnection modes of microgrids are grid-connected and islanded/stand-alone/off grid. The microgrid controller has to handle connection and disconnection between these modes [6-7]. The controller is a key to discover the entire potential of microgrids.

Microgrids have commonly three control levels namely primary, secondary, and tertiary [5, 8]. The primary level has a main task to control the distributed generator (DG) units, which is also called distributed energy resource, in a microgrid including the conversion process of voltage and current to different wave form. In order to ensure the power quality of the DG units involved in the microgrids, the secondary control level has to deal with the improvement of the performance. Power exchange between microgrids and also with the main grid is arranged by tertiary control level.

The control approach in this paper will focus on the voltage and frequency control on a single DG unit which has a DC voltage source in a microgrid by considering the dynamics in DC to three-phase AC converter, set-point changes and load uncertainties. Islanded microgrid control is more challenging compared to the grid-connected mode. In the grid-connected mode, the main grid

normally regulates voltage and frequency in microgrids, but at sudden power mismatches, the DG unit has to control them independently. The power mismatch can make a relatively high circulating current, therefore the DG Unit controller has to ensure accurate load sharing mechanism in a microgrid system. The control design by operating an inverter for DC to AC conversion as a master unit to regulate the voltage in a microgrid is a possible approach [9], while an internal oscillator controls the frequency according to the standard. Some previous approaches regarding the power sharing in microgrids can be seen in [10-16], energy management with different source types in [17-18], and also more detail reviews in [5, 19]. Moreover, to deal with interconnection of different layers, a hierarchical control system approach should be taken into account [20-21].

The voltage control in an islanded microgrid is challenging because of load parameter uncertainties, unbalanced phase, and transients. Some control approaches have been proposed to face these challenges: sliding mode [22], μ-synthesis [23], fuzzy logic [24, 25], Fuzzy-PI [26], robust [27-29], robust servomechanism [30], and convex optimization [31]. Moreover, electronic devices as additional features of voltage regulation should be added [32].

The mentioned approaches for voltage regulation developed mathematical models from parameters value of the plant such as resistance, capacitance and inductance, which may difficult to be estimated, unknown, or subject to variation. The control techniques should be kept as simple as possible to be comprehensive for the practitioners regarding how to keep the highest performance according to the system requirements. These aspects are important because some types of controller and operators might be involved once the microgrids are using some kinds of DG. The main goal of the controller is to achieve the best power quality. The controller has to guarantee the best set point tracking capability under parametric uncertainty and the satisfactory frequency.

This paper presents an approach that modifies the proportional-integral-derivative (PID) control scheme to be integral-proportional-derivative (I-PD) for regulating three-phase voltage in an islanded microgrid that has one DG unit with DC source. A transformation technique, *a-b-c* to *d-q* axis voltages and vice versa, is used to transform the three-phase voltage of the system as the real condition to DC-like waveform consisting *d*- (active) and *q*- (reactive) axis voltages. The *d-q* form will be used for designing the controller. Then, the control signal will be transformed back to *a-b-c* axis voltages. The mathematical model in *d-q* axis voltages that has multiple input and

multiple output (MIMO) form is generated by using a system identification technique. By using the estimation technique in system identification, the linear model of the microgrid system can easily generated and the order of the system can be reduced significantly compared to the manual mathematical model generation. Two linear controllers are then possible to be designed in *d-q* axis voltages.

II. SYSTEM DESCRIPTION

A high level semantic in Figure 1 represents an islanded microgrid with a DG unit that is discussed in this paper. In grid-connected mode, the point of common coupling (PCC) connects microgrid to the main grid with voltage magnitude V_{abc}. The exchange between the microgrid and the main-grid can be performed when the real and reactive power between them are zero [30]. Once the microgrid is off-grid, it turns the system into the islanded mode and causes a power gap between DG unit and the load that leads to significant frequency and voltage deviation from their rated values due to the lack of controller. The off-grid condition must be detected to maintain operation of the system uninterruptedly, while microgrid controller has to regulate independently voltage and frequency in the islanded mode.

The DG unit has a DC voltage source 1,500 V. It is converted to three-phase AC voltage by using an inverter VSC. Output of the inverter is connected to the three-phase LCL filter to improve sinusoidal waveforms quality of the three-phase voltage. Then, the three-phase voltage magnitude steps-up through a transformer in the islanded mode and supply the loads, while in the grid-connected mode the load will be supplied by the main grid. In this paper, the microgrid supply a three-phase parallel RLC load as the worst load type for common islanded detection mode methods [33-34]. The system load is 10 kW parallel RLC load at the beginning, and at 1.4s it is doubled. The controller outputs in *d-q* axis voltages (u_1 and u_2) are transformed to *a-b-c* axis voltage and connected as reference to the 2-level PWM that will produce a three-phase gate signal for the inverter. This signal is dynamics and applied to control V_{abc} magnitude in order to have the best tracking capability. V_{abc} is transformed back to *d-q* axis voltages as feedback signals to the controllers. Table I provides parameter values of the islanded microgrid discussed in this paper.

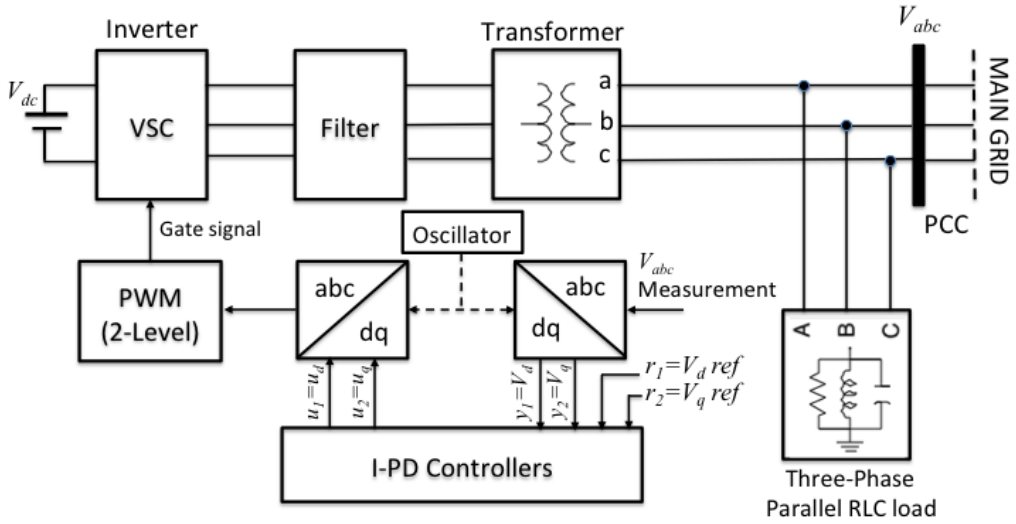

Figure 1. High level semantic of an islanded microgrid

Table 1: Islanded microgrid parameter rated values

Components	Details
Pulse-Width Modulation (PWM)	Unsynchronized Operation mode, 3 phases, 6 pulses, 2 kHz switching frequency
DG Unit Source	V_{dc} = *1500 V*
Inverter	VSC with 3 bridge arms
Filter (LCL)	R at input inductor = 0.1 Ω; L of the filter input = 0.3 μH; R at capacitor = 1 mΩ; C of the filter = 9 μF; R at output inductor = 0.1 Ω; L of the output filter = 0.3 μH
Transformer	Three single-phase, Δ-Y connection, 110 kVA Nominal Power, Frequency 50 Hz, V_{rms} at primary side = 600 V, V_{rms} at secondary side = 13.8 kV, base power 110 KVA (three-phase)
Basic Load	Three- phase parallel RLC load, Nominal frequency = 50 Hz, Active Power = 10 kW, Inductive reactive power = 5 var, Capacitive reactive power = 5 var

Intermittent characters of DG units where the renewable source connected directly to the system without battery will affect the inverter and subsequently the islanded microgrid. In this paper, the DC source is assumed having a fixed nominal voltage, which is 1,500 V. The voltage magnitude

set-point changes in the islanded mode can affect stability and robustness of the system performances especially voltage and frequency. Two I-PD controllers regulate V_{abc} and phase-locked loop (PLL) units as internal oscillators pre-determine frequency and phase of current and voltage of the islanded microgrid. The controller design objective is to improve and to maintain the quality of voltage magnitude and frequency in the islanded microgrid in order to face set-point changes and load uncertainty. Set-point tracking performance is the indicator of the good performance.

III. UNCOMPENSATED ISLANDED MICROGRID

Figure 2 presents the uncompensated real system (non-linear) model of an islanded microgrid that has a DG unit. The outputs of non-linear and linear model are investigated to make sure the mathematical model generated by system identification for block diagram of the control system closely represents the real system. Then, the goal is to provide a control strategy for the voltage and frequency regulation based on IEEE recommendation [33-34]. The nominal value of V_{abc} is 13.8 kV with base power 110 KVA (three-phase). The controllers have to maintain that V_{abc} deviation maximum 10% of the nominal value and do not have swell (V_{abc} is 1.1 V_{abc} for 0.5 cycles to one minute) and dip/sag ($0.9V_{abc}$ for 0.5 cycles to one minute). Total harmonic distortion (THD) of voltage shall no greater than 5 %. For the transition, the maximum overshoot of voltage shall be less than 1.4 nominal value, the rise time less than 0.02 s, the settling time no greater than 1 s. Impulsive transients should have peak between 10 – 50 % V_{abc}. Besides, the frequency deviation allowed is 0.2 Hz.

Transformation the three-phase voltage to a stationary α-β axis coordinates and subsequently to a rotating *d*-*q* axis coordinates makes away to have a linear model representation. It is hard to design a simple linear controller without approximation if the system dynamics are nonlinear in the *a*-*b*-*c* and α-β axis voltages. In the *d*-*q* axis voltages, the dynamics are approximately linear, making linear controller design much easier. In Figure 2, u_1 and y_1 represent the *d*-axis voltage for input and output respectively, and u_2 and y_2 for *q*-axis voltage. An example of using *d*-*q* axis voltage concerning three-phase voltage and current signals for anti-windup compensator design is presented in [35]. Transforming controller output from *d*-*q* to *a*-*b*-*c* axis voltages for the input of the 2-level PWM results a gate signal to the inverter. It will then control subsequently the inverter

output, and V_{abc} and frequency. The PLL determines the frequency of the islanded microgrid according to the standard (i.e. 50 Hz). Initially, the system has three-phase parallel RLC load with 10 kW active power and 13.8 kV nominal phase-to-phase voltage (*Vrms*). The nominal voltage decreases 40% at 0.7 s and returns to 13.8 kV again at 1.2 s. The RLC load will be doubled at 1.4 s once the circuit breaker is closed.

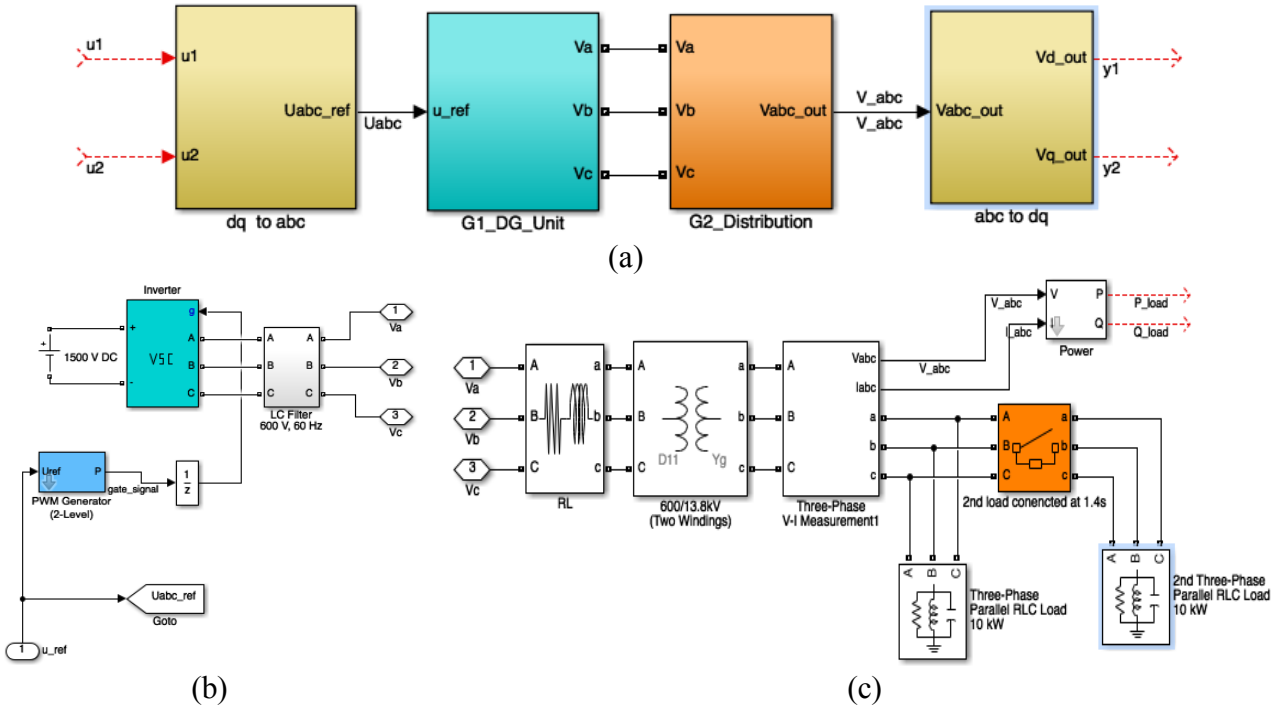

Figure 2. Uncompensated real system (non-linear) model: (a) main model, (b) G1_DG_Unit block, (c) G2_Distribution Block

In real situations, finding mathematical model of the system is difficult to be done since there is always lack of the technical information and the system used to involve high uncertainty and nonlinearity. In the controller design, the transfer functions estimation of the plant are generated by system identification. It conceals some details but more reliable in real condition in the electrical systems. Three parameters considered choosing size of numerators and denumerators of the transfer functions are fit percent to estimation data (FP), Akaike's final prediction error (FPE) and mean square error (MSE). The best size is determined based on the FP, FPE and MSE as well as the stability of the open-loop transfer functions.

The plant model (*Gp*) of the islanded microgrid in Figure 2 has four transfer functions in MIMO structure where all them are asymptotically stable. Four transfer functions in equation show the mathematical model of the plant. Table 2 shows the estimation properties of the transfer functions. Both *d-q* axis coordinates affect each other because of the coupling effect through Gp_{12} and Gp_{21}. In the closed-loop system, this effect can influence the system if the error in each axis is big. Therefore, Gp_{12} and Gp_{21} have to be taken into account. The uncompensated system is asymptotically stable but lacks set point tracking capability and robustness.

$$y_1(s) = Gp_{11}(s)u_1(s) + Gp_{12}(s)u_2(s)$$
$$y_2(s) = Gp_{21}(s)u_1(s) + Gp_{22}(s)u_2(s)$$
$$where,$$
$$Gp_{11}(s) = \frac{-275.3\ s + 1{,}643{,}000}{s^2 + 3{,}597s + 887{,}400};\quad Gp12(s) = \frac{342.6\ s + 84{,}880}{s^2 + 273.3\ s + 78{,}900} \tag{1}$$
$$Gp21(s) = \frac{-345.9\ s - 84{,}530}{s^2 + 275.6\ s + 78{,}570};\quad Gp22(s) = \frac{-326.1\ s + 1{,}778{,}000}{s^2 + 3{,}876s + 960{,}600}$$

Table 2: Estimation properties for the transfer functions in equation (1)

Transfer Function	**Estimation Properties**			
	FP (%)	**MSE**	**FPE**	**(Numerator, Denumerator)**
Gp_{11}	96.94	0.003124	0.003124	(2,2)
Gp_{12}	95.01	0.002922	0.002922	(2,2)
Gp_{21}	95.07	0.002856	0.002856	(2,2)
Gp_{22}	96.94	0.003112	0.003112	(2,2)

IV. CONTROLLER DESIGN

In the controller design, the open-loop characteristics of the system have been examined. Load uncertainties might perturb the voltage and frequency. The total load allowed in the system should be less than the base power (i.e. 110 KVA). In the simulation, the first load connected to the system is 10 kW and another 10 kW added at 1.4 s. The coupling effects through *Gp12* and

Gp21 should be decreased to minimize the errors. Figure 3 shows a comparison of responses between real system (non-linear) and linear model using a unit-step input as set point for *d*-axis voltage and a zero signal for *q*-axis voltage. The uncompensated system obviously lacks set point tracking capability with large steady state error and overshoot.

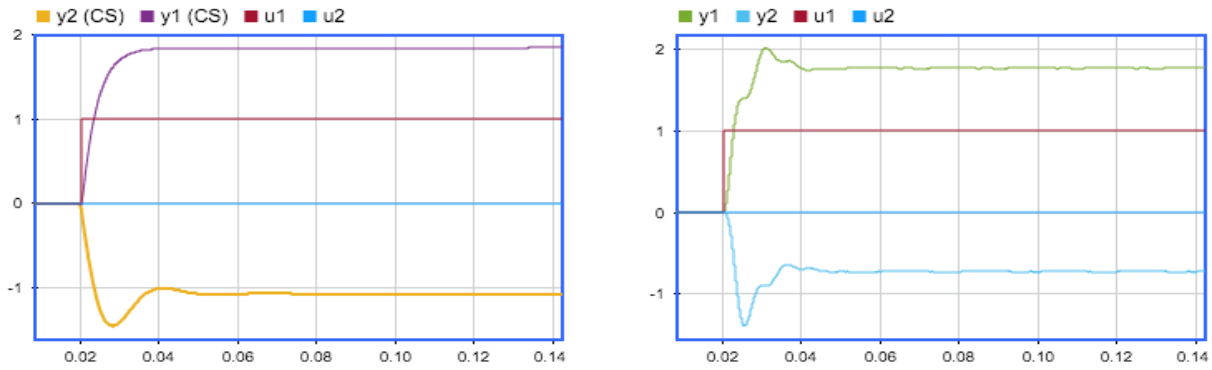

(a) (b)

Figure 3. Uncompensated system responses: (a) linear model, (b) non-linear model

a. Control System Requirements

The controller design is an effort to fulfill the system requirements. It has to make sure that controller can be designed and analyzed by using linear time invariant (LTI) system tools and methods. The requirements mentioned in section III regarding the power quality are then transformed into pu (per unit) dimension. The pu value represents the dimensionless ratio of the original quantity to its base value. The control design requirements are as follows:

- *d*-axis voltage reference (r_1) is firstly set 1 pu and then 0.6 pu at 0.7 s and return to 1 pu at 1.2 s,
- *q*-axis voltage reference (r_q) is always zero,
- Rise time < 0.2 s, settling time < 1 s, and maximum overshoot < 0.2 pu.
- Impulsive transient peak < 0.5 pu.
- In steady state, voltage deviation is 0.1 pu and THD of each phase of *a-b-c* coordinate less than 5 %.
- The closed-loop systems are asymptotically stable,
- The system should capable of maintaining the frequency with only 0.2 Hz deviation allowed,

- The controller is desired to be robust for the range of RLC load parameters.
- 1 pu voltage equals to 13.8 KV
- 1 pu power equals to base power 110 KVA

b. Proposed Controller Design

I-PD controller is a modification of PID control scheme [36]. In I-PD scheme, derivative and proportional action are put directly to the feedback path. It is purposed to prevent large control signals that can cause saturation. The I-PD controller is a single input single output (SISO) method applied in the presented islanded microgrid to control the *d-q* axis voltages. The system has a 2 x 2 (MIMO) structure, but two I-PD controllers are tuned on a SISO manner, since the coupling effect between *d*- and *q*- axis is relatively small.

The tune method for the I-PD parameters has applied first rule of Ziegler-Nichols since the open-loop system response revealed S-shape curve. The delay time (L) and time constant from the delay to settling time (T) have been used to calculate the constant of proportional gain (K_p), integral time (T_i) and derivative time (T_d). Similar S-shape of both *d-q* axis voltages at the uncompensated system is the reason of L and T having same values. Two I-PD controllers set L=0.003 and T=0.0067. The control parameters are as follows,

$$\begin{aligned} &K_{p1} = K_{p2} = 1.2(T/L) = 2.68; \\ &T_{i1} = T_{i2} = 2L = 0.006; \\ &T_{d1} = T_{d2} = 0.5L = 0.0015; \end{aligned}$$

$$\begin{aligned} &Y = (I - KG_P)^{-1} KG_P FR = G_{cl} R \\ &K = \begin{bmatrix} K1 & 0 \\ 0 & K2 \end{bmatrix};\ G_P = \begin{bmatrix} Gp11 & Gp12 \\ Gp21 & Gp22 \end{bmatrix};\ F = \begin{bmatrix} F1 & 0 \\ 0 & F2 \end{bmatrix}; \\ &G_{cl} = \begin{bmatrix} Gcl11 & Gcl12 \\ Gcl21 & Gcl22 \end{bmatrix}; \\ &K1 = K_{p1}(1 + (1/T_{i1}s) + T_{i1}T_{d1}s^2); \qquad K2 = K_{p2}(1 + (1/T_{i2}s) + T_{i2}T_{d2}s^2); \\ &F1 = \frac{1}{1 + T_{i1}s + T_{i1}T_{d1}s^2}; \qquad F2 = \frac{1}{1 + T_{i2}s + T_{i2}T_{d2}s^2}; \end{aligned} \tag{3}$$

Equation (3) presents the closed-loop (compensated) model of the islanded microgrid, while Figure 4 shows its representation in non-linear model in MATLAB software environment. The I-PD control scheme has a quite similar structure with ideal PID, but it has filter (F) at the reference (R). The compensated system applies I-PD controllers to improve the tracking capability. The coupling effects of $Gp12$ to output y_1 and $Gp21$ to output y_2 have been taken into account in the model. By reducing the errors to zero, their effects decrease to zero as well.

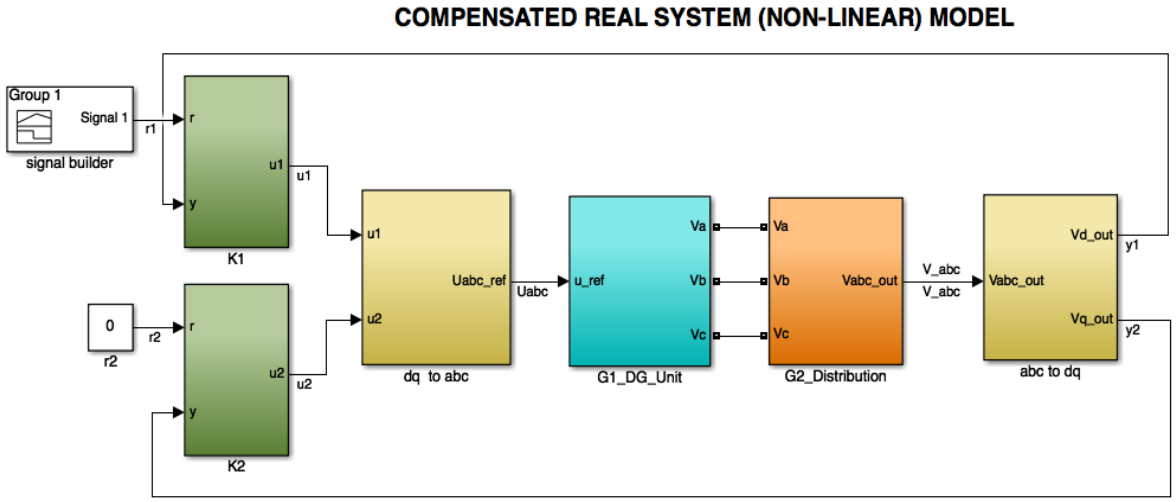

Figure 4. Compensated non-linear system model in MATLAB software environment

c. Simulation-based Analysis of the compensated System

Figure 5 shows unit-step responses of the compensated system at the transition by comparing I-PD and PID control scheme either in the linear (LTI) or non-linear model. Meanwhile, Figure 6 depicts the system response with dynamic set point. Both figures confirm that I-PD controller is superior compared to PID. System compensated with I-PD controller shows a very good set-point tracking capability and robustness of the system. The PID gives more oscillation in the system response than I-PD. In the real system (non-linear) model, the I-PD controller can reduce the peak of the transient according to standard.

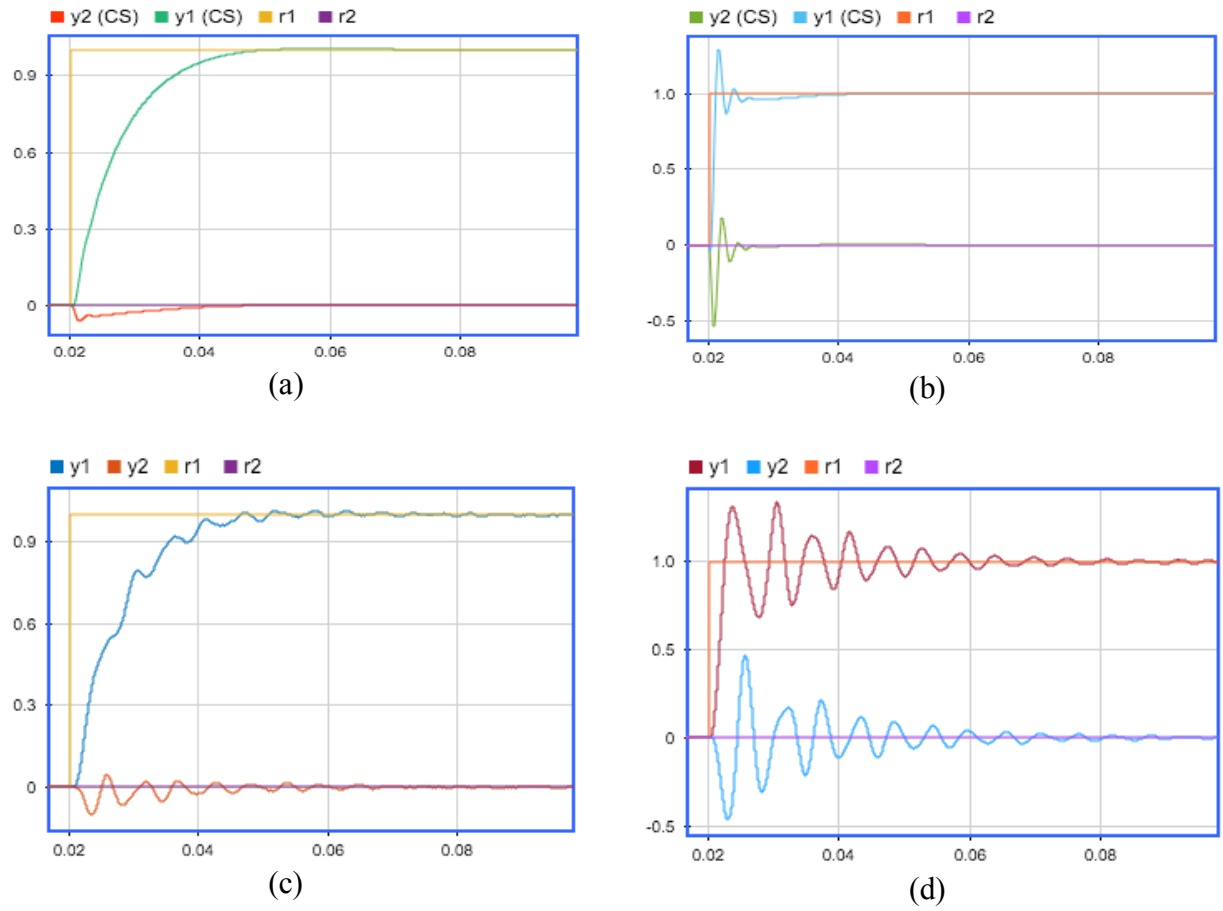

Figure 5. Unit-step transient responses of the compensated system: (a) I-PD Control in linear model, (b) PID control in linear model, (c) I-PD control in non-linear model, (d) PID control in non-linear model.

IV. PERFORMANCE ANALYSIS: A CASE STUDY

A case study is undertaken to investigate the performance of the compensated system based on the IEEE recommendation [33-34]. At the beginning, the voltage set point is 1 pu, then decreases to 0.6 pu at 0.7s. It will return to 1 pu at 1.2 s. The set point drop may happen when there is a large starting current in short duration. In most cases, starting of motors can cause adverse effects to any locally connected load, even they are electrically remote from the point of motor starting [37]. At time of starting, the voltage induced in the induction motor rotor is maximum because slip will be maximum, where since the rotor impedance is low, the rotor current is excessive large

[37]. Due to transformer action this large rotor current is reflected in the stator [38]. This results in large starting current, nearly 6 to 8 times [37], or 5 to 6 times [39-40] the full-load current in the stator. This large current does not harm the motor due to short duration. However, this large starting current will produce large drop in line-voltage [37]. The more motor as a load, the larger voltage drop in the line-voltage would be.

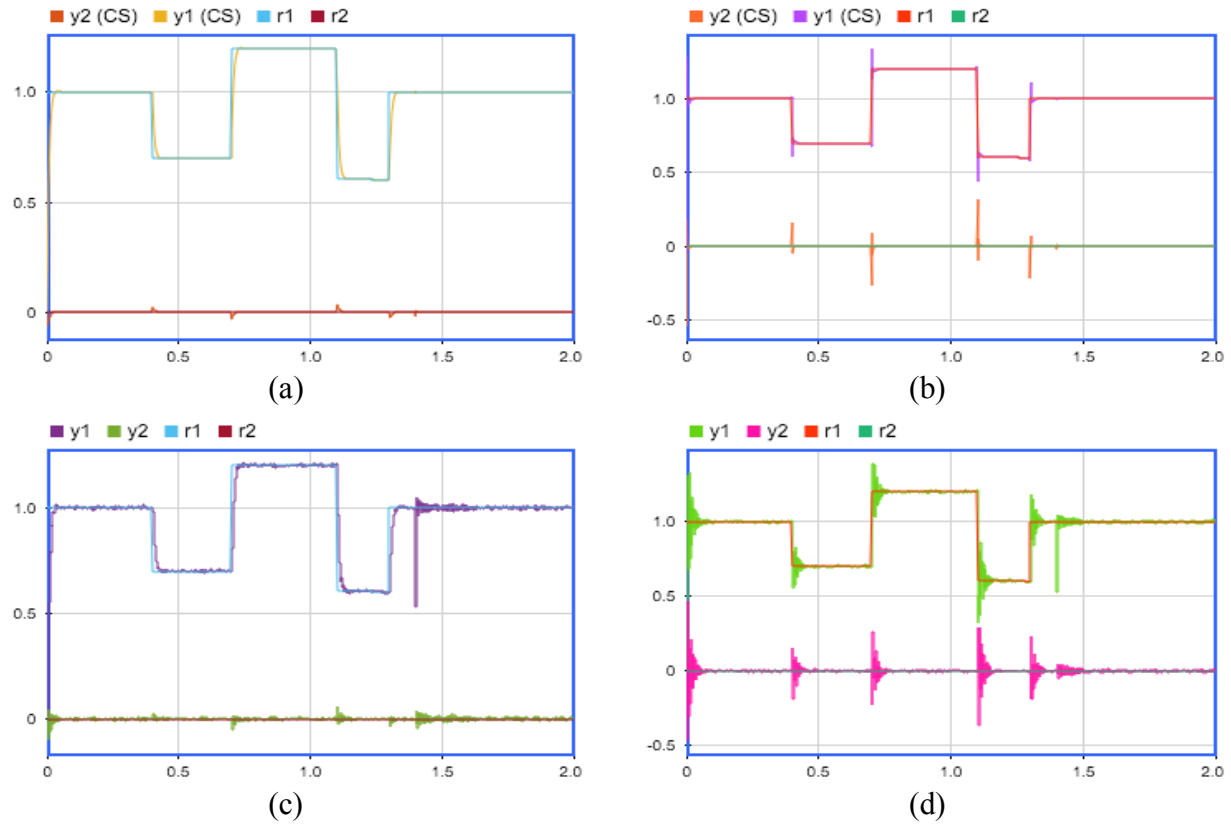

Figure 6. Responses of the compensated system with dynamic set-point: (a) I-PD Control in linear model, (b) PID control in linear model, (c) I-PD control in non-linear model, (d) PID control in non-linear model.

Furthermore, in the present system, the load is doubled at 1.4s. Figure 7 shows the responses related to the case study for the whole duration of simulation time (i.e. 2 s) in *a-b-c* axis coordinates for V_{abc} (with the magnitude reference according to the case, *r1*), I_{abc}, P_{load}, and Q_{load}. When the load doubled, the voltage can be regulated while the current increases about 100%. P_{load} and Q_{load} show similar responses. Further detail in transition, voltage set-point drop, and voltage set-point return to 1 pu and load doubled can be seen respectively in Figure 8-10. In the

transition (Figure 8), settling time is about 0.02 s, which fulfills the requirement. Rise time and maximum overshoot also meet the requirements

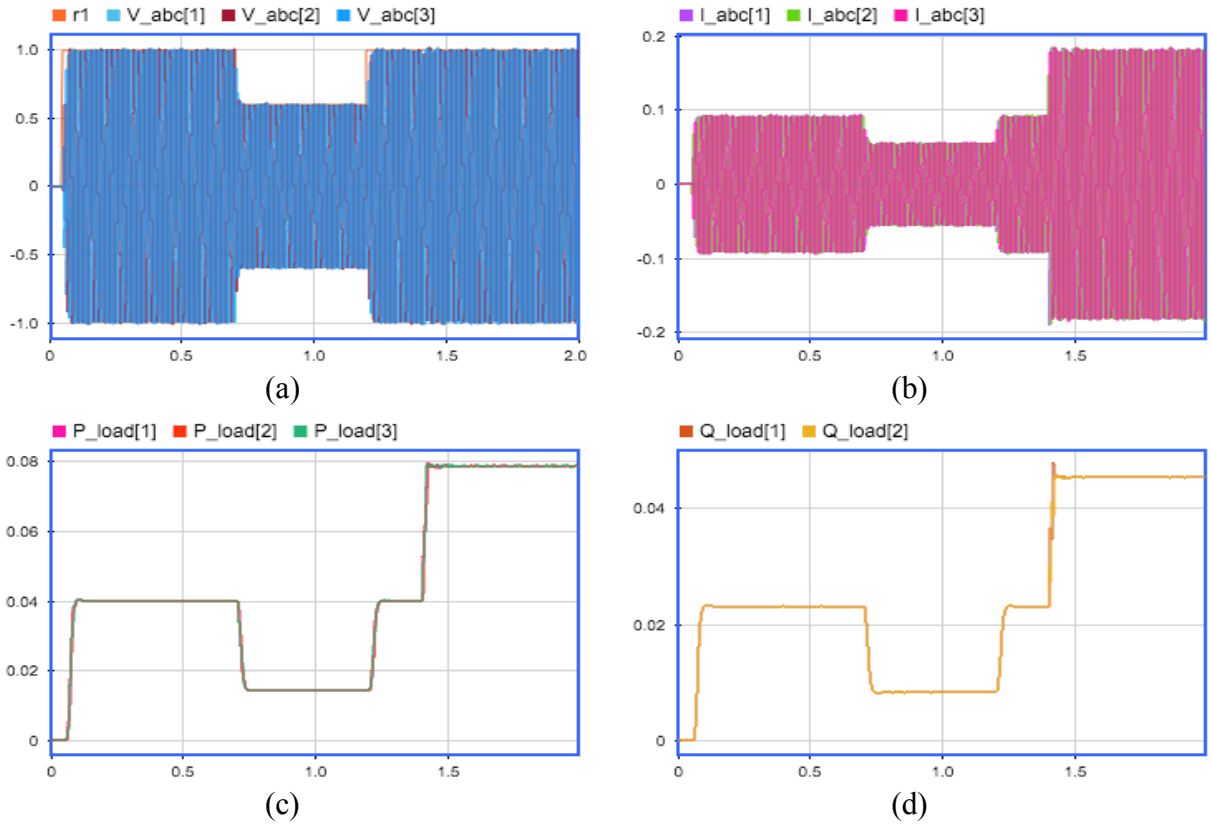

Figure 7. Electrical signal responses of the system I-PD control with set-point and load changes: (a) Three-phase voltage (V_{abc}), (b) Three-phase current (I_{abc}), (c) Active Power (P), and Reactive Power (Q)

An impulse transient peak at 1.4 s is about a 0.4 pu for *d*-axis voltage and 0.02 for *q*-axis voltage, or *0.307* for *d-q* axis, which meets the standard (< 0.5 pu). Beside the voltage deviation is close to zero, frequency of V_{abc} is always 50 Hz since it is set internally using PLL. The THD values for three-phase voltage in steady state condition are 0.5665%, 0.3564% and 0.3530% that fulfill the standard (< 5%). The compensated system shows a very good performance even in the real system model simulation. In the simulation, the system reveals no long duration rms variations of interruption, under-voltage, over-voltage, and also sag and swell even at the load parameter changes.

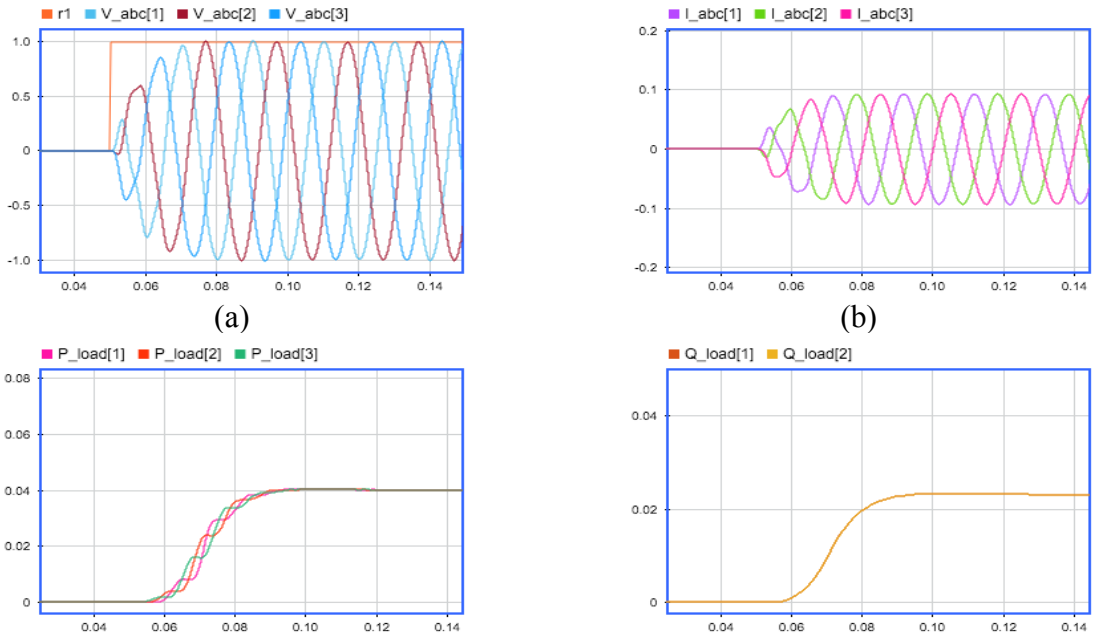

Figure 8. Electrical signal transition time responses of the system with I-PD control: (a) Three-phase voltage (V_{abc}), (b) Three-phase current (I_{abc}), (c) Active Power (P), and Reactive Power (Q)

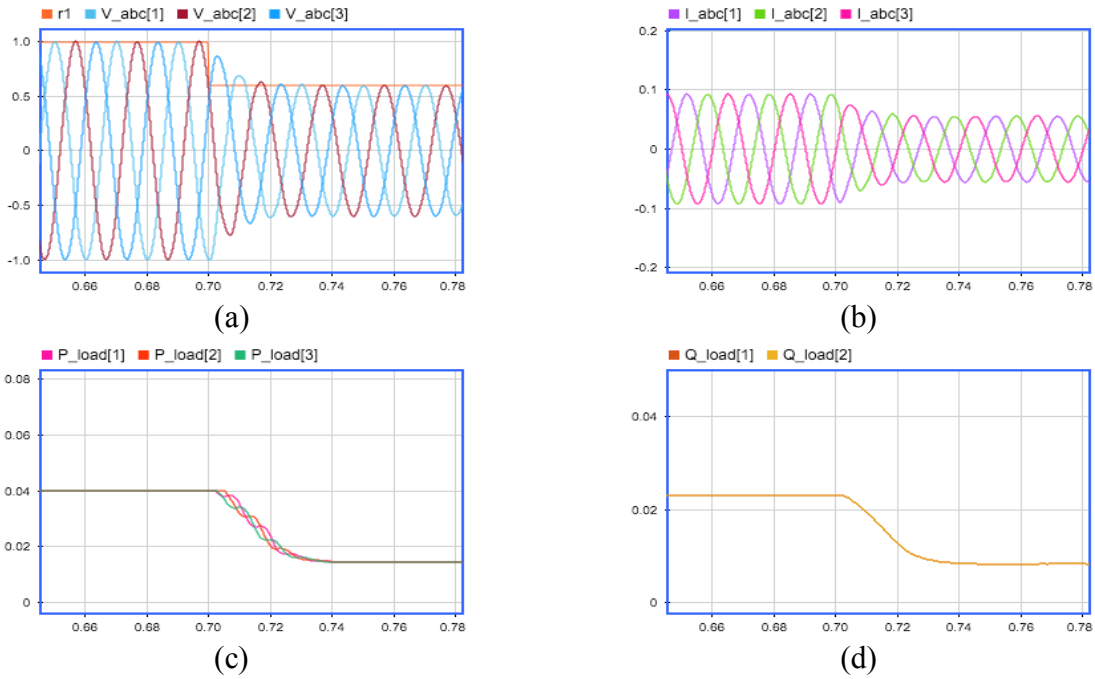

Figure 9. Electrical signal transition time responses of the system with I-PD control at set-point changes: (a) Three-phase voltage (V_{abc}), (b) Three-phase current (I_{abc}), (c) Active Power (P), and Reactive Power (Q)

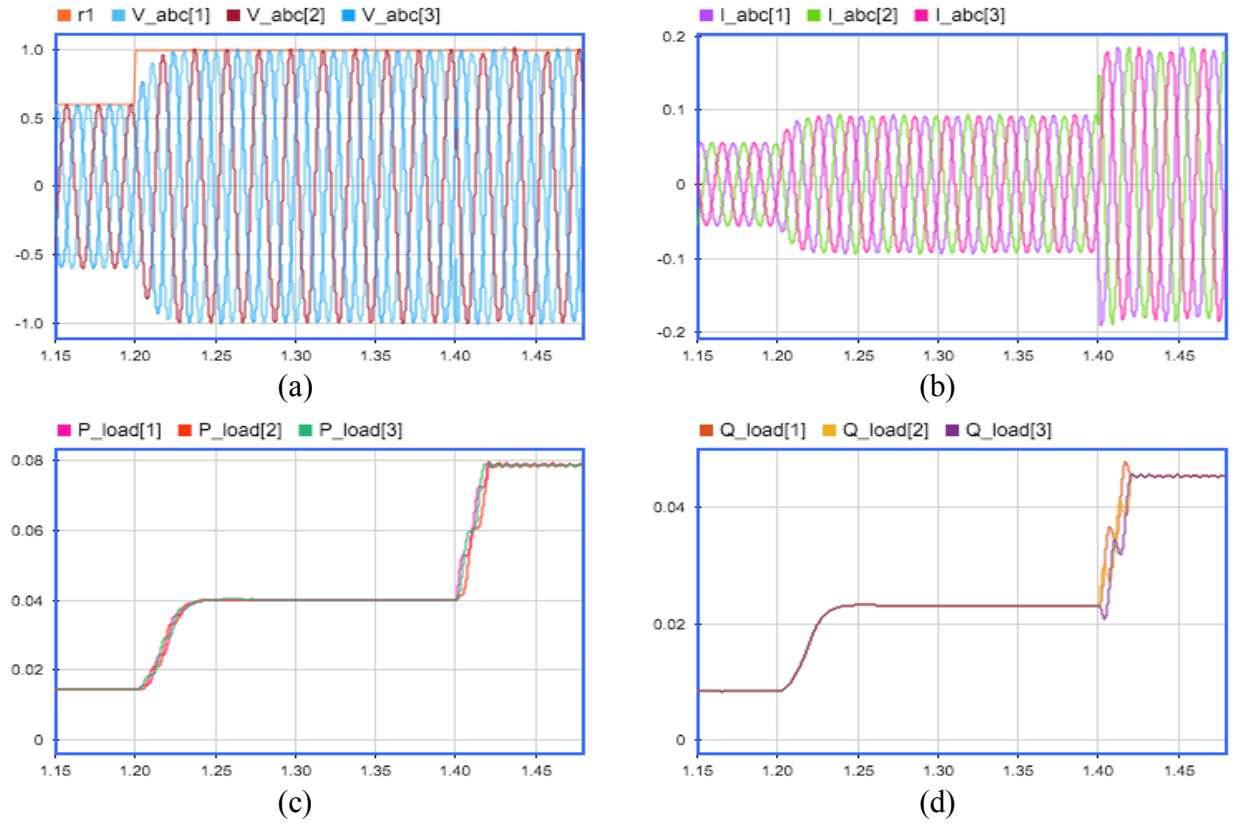

Figure 10. Electrical signal transition time responses of the system with I-PD control at load increase double: (a) Three-phase voltage (V_{abc}), (b) Three-phase current (I_{abc}), (c) Active Power (P), and Reactive Power (Q)

IV. CONCLUSIONS

This paper has elucidated a dynamic model and a controller design to regulate the voltage and frequency in an islanded microgrid with a DG unit. The dynamic model is represented as a linear model based on transfer functions of the DG unit and the load in *d-q* axis voltages generated by an estimation technique. I-PD controllers as modification of PID control scheme are proposed to control the *d-q* axis voltages connected to a gate signal of the interface inverter of the DG unit. The performance of the proposed controllers is evaluated based on the IEEE standard through the simulation studies in MATLAB. The compensated system responses show a very good set point tracking capability, robustly maintain the voltage magnitude and frequency, and involve system dynamics. The next work addresses energy management between DG units and microgrids by developing the scheduling and distributed control technique in [41].

ACKNOWLEDGEMENT

The authors thank to DRPM RistekDikti Indonesia for the research funding through PKLN research scheme, and also to Tanjungpura University and University of Leicester that facilitated and support the research especially for administration and workplaces.

REFERENCES

[1] P. Visconti, A. Lay-Ekuakille, P. Primiceri, and G. Cavalera, "Wireless Energy Monitoring System of Photovoltaic Plants with Smart Anti-Theft Solution Integrated with Control Unit of Household Electrical Consumption," International Journal on Smart Sensing and Intelligent Systems, Vol. 9, No. 2, pp. 681-708, June 2016.

[2] Y. Zhao, V. Gies, and J. Ginoux, "WSN based Thermal Modeling: A New Indoor Energy Efficient Solution," International Journal on Smart Sensing and Intelligent Systems, Vol. 8, No. 2, pp. 869-895, June 2015.

[3] S.D. Panjaitan and A. Hartoyo, "A lighting control system in buildings based on fuzzy logic," TELKOMNIKA, Vol. 9, No. 3, pp. 423-432, April 2013.

[4] S.D. Panjaitan, N. Fratama, A. Hartoyo, and R. Kurnianto, "Telemonitoring Temperature and Humidity at Bio-energy Process using Smart Phones," TELKOMNIKA, Vol. 14, No.2, pp. 762-771, June 2016.

[5] D.E. Olivares, A. Mehrizi-Sani, A.H. Etemadi, C.A. Canizares, R. Iravani, M. Kazerani, A.H. Hajimiragha, O. Gomis-Bellmunt, M. Saeedifard, R. Palma-Behnke, G.A. Jimenez-Estevez, and N.D. Hatziargyriou, "Trends in microgrid control," IEEE Trans. Smart Grid, vol. 5, pp. 1905-1919, July 2014.

[6] F. Katiraei, M.R. Iravani, and P.W. Lehn, "Micro-grid autonomous operation during and subsequent to islanding process," IEEE Trans. Power Delivery, vol. 20, pp. 248-257, Jan. 2005.

[7] H. Karimi, H. Nikkhajoei, and R. Iravani, "Control of an electronically-coupled distributed resource unit subsequent to an islanding event," IEEE Trans. Power Delivery, vol. 23, pp. 493-501, Jan. 2008.

[8] H. Bevrani, M. Watanabe, and Y. Mitami, Power system monitoring and control, John Wiley & Sons, Inc., 2014.

[9] J.A.P. Lopes, C.L. Moreira, and A.G. Madureira, "Defining control strategies for microGrids islanded operation," IEEE Trans. Power Systems, vol. 21, pp. 916-924, May 2006.

[10] M.B. Delghavi and A. Yazdani, "An adaptive feedforward compensation for stability enhancement in droop-Controlled inverter-Based microgrids," IEEE Trans. Power Delivery, vol. 26, pp. 1764-1773, July 2011.

[11] P. Li, X. Wang, W. Lee, and D. Xu, "Dynamic power conditioning method of microgrid via adaptive inverse control," IEEE Trans. Power Delivery, vol. 30, pp. 906-913, April 2015.

[12] M.J. Hossain, H.R. Pota, M.A. Mahmud, and M. Aldeen, "Robust control for power sharing in microgrids with low-inertia wind and PV generators," IEEE Tran. Sustain. Energy, vol. 6, pp. 1067-1077, July 2015.

[13] Q. Zhong and G. Weiss, "Synchronverters: inverters that mimic synchronous generators," IEEE Trans. Industrial Electronics, vol. 58, pp. 1259-1267, April 2011.

[14] Q. Zhong, G. Konstantopoulos, B. Ren, and M. Krstic, "Improved synchronverters with bounded frequency and voltage for smart grid integration," IEEE Trans. Smart Grid, Vol. PP, No. 99, 2017.

[15] H. Zhang, S. Kim, Q. Sun, and J. Zhou, "Distributed Adaptive Virtual Impedance Control for Accurate Reactive Power Sharing Based on Consensus Control in Microgrids," IEEE Transactions on Smart Grid, vol. 8, no. 4, pp. 1749-1761, July 2017.

[16] Y. S. Kim, E. S. Kim, and S. I. Moon, "Distributed Generation Control Method for Active Power Sharing and Self-Frequency Recovery in an Islanded Microgrid," IEEE Trans. on Power Systems, vol. 32, no. 1, pp. 544-551, Jan. 2017.

[17] X. Sun, B. Liu, Y. Cai, H. Zhang, Y. Zhu, and B. Wang, "Frequency-based power management for photovoltaic/battery/fuel cell-electrolyser stand-alone microgrid," IET Power Electronics, vol. 9, no. 13, pp. 2602-2610, October 2016.

[18] L. Guo, W. Liu, X. Li, Y. Liu, B. Jiao, W. Wang, C. Wang, and F. Li, "Energy Management System for Stand-Alone Wind-Powered-Desalination Microgrid," IEEE Transactions on Smart Grid, vol. 7, no. 2, pp. 1079-1087, March 2016.

[19] S.M. Ashabani and Y.A.I. Mohamed, "New family of microgrid control and management strategies in smart distribution grids-analysis, comparison and testing," IEEE Trans. Power Systems, vol. 29, pp. 2257-2269, Sept. 2014.

[20] Y.A.I. Mohamed and A.A. Radwan, "Hierarchical control system for robust microgrid operation and seamless mode transfer in active distribution systems," IEEE Trans. Smart Grid, vol. 2, pp. 352-362, June 2011.

[21] Y. Han, P. Shen, X. Zhao, and J. M. Guerrero, "Control Strategies for Islanded Microgrid Using Enhanced Hierarchical Control Structure With Multiple Current-Loop Damping Schemes," IEEE Trans. on Smart Grid, vol. 8, no. 3, pp. 1139-1153, May 2017.

[22] M. Cucuzzella, G.P. Incremona, and A. Ferrara, "Design of robust higher order sliding mode control for microgrids," IEEE J. on Emerging and Selected Topics in Circuits and Systems, vol. 5, pp. 393-401, Sept. 2015.

[23] M. Babazadeh and H. Karimi, "μ-synthesis control for an islanded microgrid with structured uncertainties," 37th Annual Conference of the IEEE Industrial Electronics Society, pp. 3064-3069, 2011.

[24] D.Q. Dang, Y. Choi, H.H. Choi, and J. Jung, "Experimental validation of a fuzzy adaptive voltage controller for three-phase PWM inverter of a standalone DG unit," IEEE Trans. Industrial Informatics, vol. 11, pp. 632-641, June 2015.

[25] H.M. Hasanien and M. Matar, "A fuzzy logic controller for autonomous operation of a voltage source converter-based distributed generation system," IEEE Trans. Smart Grid, vol. 6, pp. 158-165, Jan. 2015.

[26] I. Sefa, N. Altin, S. Ozdemir, and O. Kaplan, "Fuzzy PI controlled inverter for grid interactive renewable energy systems," IET Renewable Power Generation, vol. 9, pp. 729-738, Sept. 2015.

[27] A.H. Etemadi, E.J. Davison, and R. Iravani, "A decentralized robust control strategy for multi-DER microgrids-part I: fundamental concepts," IEEE Trans. Power Delivery, vol. 27, pp. 1843-1853, Oct. 2012.

[28] M. Babazadeh and H. Karimi, "Robust decentralized control for islanded operation of a microgrid," IEEE Power and Energy Society General Meeting, pp. 1-8, 2011.

[29] A. Kahrobaeian and Y.A.I. Mohamed, "Suppression of interaction dynamics in DG converter-based microgrids via robust system-oriented control approach," IEEE Trans. Smart Grid, vol. 3, pp. 1800-1811, 2012.

[30] H. Karimi, E.J. Davison, and R. Iravani, "Multivariable servomechanism controller for autonomous operation of a distributed generation unit: design and performance evaluation," IEEE Trans. Power Systems, vol. 25, pp. 853-865, May 2010.

[31] B. Bahrani, M. Saeedifard, A. Karimi, and A. Rufer, "A multivariable design methodology for voltage control of a single-DG-unit microgrid," IEEE Trans. Industrial Informatics, vol. 9, pp. 589-599, May 2013.

[32] A.H. Etemadi and R. Iravani, "Overcurrent and overload protection of directly voltage-controlled distributed resources in a microgrid," IEEE Trans. Industrial Electronics, vol. 60, pp. 5629-5638, Dec. 2013.

[33] IEEE PES Society, "IEEE recommended practice for monitoring electric and power quality", IEEE Standard 1159TM – 2009.

[34] IEEE, "Standard for interconnecting distributed resources with electric power systems", IEEE Standard 1547– 2003.

[35] P. March and M.C. Turner, "Anti-windup compensator design for nonsalient permanet-magnet synchronous motor speed regulators," IEEE Trans. Industry Applications, Vol. 45, no. 5, pp. 1598-1609, Sept. 2009.

[36] K. Ogata, Modern control engineering, fifth Edition, Prentice Hall, Pearson, 2010.

[37] T. Wildi, "Electrical Machines, Drives and Power Systems", 6th Edition, Pearson Education Limited, August 2013.

[38] H. Hu, C.X. Mao, M.L. Ji, and Y.X. Yu, "The torque oscillation study in the motor soft starting process with discrete variable frequency method", International Conference on Electrical Machines and Systems (ICEMS), pp. 1686-1690, 2008.

[39] I.J. Nagrath and D.P. Kothari, "Electric Machines", 2nd Edition, Tata McGraw-Hill Publishing Company Limited, New Delhi, 2006.

[40] A. Garge and A. Tomar, "Starting Time Calculation for Induction Motor", J. Electr. Electronic System, vol. 4, no. 149, 2015.

[41] S.D. Panjaitan, "Development process for distributed automation systems based on elementary mechatronic functions," Shaker-Verlag, Aachen-Germany, 2008.